Controlled enhancement of spin current emission by three-magnon splitting

Hidekazu Kurebayashi*[1], Oleksandr Dzyapko[2], Vlad E. Demidov[2], Dong Fang[1], Andrew J. Ferguson[1] and Sergej O. Demokritov[2]

[1] *Cavendish Laboratory, University of Cambridge, J. J. Thomson Avenue, CB3 0HE, UK.*

[2] *Institute for Applied Physics, University of Muenster, Corrensstr. 2-4, 48149 Muenster, Germany*

**Correspondence should be addressed to hk295@cam.ac.uk*

Spin currents, the flow of angular momentum without the simultaneous transfer of electrical charge, play an enabling role in the field of spintronics[1-8]. Unlike the charge current, the spin current is not a conservative quantity within the conduction carrier system. This is due to the presence of the spin orbit interaction that couples the spin of the carriers to angular momentum in the lattice. This spin-lattice coupling[9] acts also as the source of damping in magnetic materials, where preccessing magnetic moment experiences a torque towards its equilibrium orientation; the excess angular momentum in the magnetic subsystem flows into the lattice. In this Letter, we show that this flow can be reversed by the three-magnon splitting process and experimentally achieve enhancement of spin current emitted by the interacting spin-waves. This mechanism triggers angular momentum transfer from the lattice to the magnetic subsystem and modifies the spin current emission. The finding illustrates the importance of magnon-magnon interactions for developing spin-current based electronics.

By using angular momentum exchanges between conduction electrons and spin waves, the long-range transport of spin current has recently been demonstrated in magnetic insulators[8], finding an important role for these materials within spin-based electronic devices. In order to create and detect the spin current, layers of a strongly spin-orbit coupled metal (Pt) were

placed on the magnetic insulator (yttrium iron garnet, YIG). Passing a current through the metal layer generates a spin current, using the spin-Hall effect (SHE)[10,11]. The spin current is injected into the magnetic dielectric, where it results in an excitation of a propagating spin wave. After propagation for a certain distance, the spin angular momentum of the spin wave is converted into a voltage in the second metal layer by using the inverse spin-Hall effect (ISHE)[7]. This signal-transmission scheme has advantages over the conceptually simpler approach of using spin-polarized electrons in conducting materials, due to the longer propagation length of spin waves compared to the spin-diffusion length in metals. While the spin diffusion length of conduction carriers in metals is normally several hundreds of nanometers[12], spin waves in magnetic dielectrics such as YIG can propagate to macroscopic distances without significant attenuation owing to very small magnetic damping in this material[13]. The performance of such a signal transmission scheme is mainly limited by the conversion efficiency of a spin current into the magnetisation precession and vice versa. Since the output voltage in this scheme is directly proportional to the spin current flowing across the interface between the magnetic dielectric and the metal film, the way to improve the performance of the scheme is to find a mechanism for an efficient enhancement of the spin current. Here we demonstrate that such enhancement can be realised by using the three-magnon splitting process, a magnon-magnon interaction in which the total angular momentum of the magnetic subsystem is not conserved. Moreover, we show that this mechanism can be switched on and off by modification of the spin-wave spectrum in YIG by the applied static magnetic field.

Figure 1a is a schematic of the studied system which consists of a bi-layer of a magnetic insulator YIG and a spin current detector Pt. We first characterise magnetic properties of the YIG film by ferromagnetic resonance (FMR) technique. Figure 1b demonstrates the

dependence of microwave absorption on the magnetic field measured for a fixed excitation frequency f=5 GHz. The absorption curve is asymmetric and exhibits a maximum at the field H_{res}. This asymmetry is most likely due to the contribution of different standing spin-wave modes[14]. The maximum of the curve corresponds to the fundamental spin-wave mode of the finite-size YIG sample being an analogue of the uniform FMR mode in an infinite ferromagnetic medium. The connection between resonant field of this mode H_{res} and the frequency f can be approximated with a good accuracy by the Kittel formula[15] $f = \gamma\mu_0\sqrt{H_{res}(H_{res}+M)}$, where γ=28 GHz/T is the gyromagnetic ratio and $\mu_0 M$ = 0.175 T is the saturation magnetisation of YIG (Fig. 1c). The voltage detected across the Pt film also shows the resonance-like behaviour with a maximum at H_{res}. To prove whether the observed voltage is actually caused by the ISHE and that it can be used as a measure of the spin current, we performed these measurements for three different directions of the static field $\boldsymbol{H}_0$, as shown in Fig. 1d. Considering the most important flow of the longitudinal magnetization (i.e. along $\boldsymbol{H}_0$), voltages arising from the ISHE follow the symmetry of conversion from a spin current $\boldsymbol{j_s}$ into electromotive force $\boldsymbol{E}$ as[7]:

$$\boldsymbol{E} = D_{ISHE}\,\boldsymbol{j_s}\times\boldsymbol{\sigma}, \qquad (1)$$

where D_{ISHE} and $\boldsymbol{\sigma}$ are the conversion efficiency and the unit vector in the direction of the spin polarization of $\boldsymbol{j_s}$, respectively. As defined in Fig. 1a, the directions of E and $\boldsymbol{j_s}$ are fixed along the y and x direction for our set-up respectively, and the direction of $\boldsymbol{\sigma}$, being parallel to $\boldsymbol{H}_0$ in the in-plane measurements, can be experimentally controlled. In agreement with Eq. (1), we observed the voltage only when $\boldsymbol{H}_0$ was applied along the z-axis with a corresponding sign change and no sizable voltage was measured for $\boldsymbol{H}_0$ parallel/antiparallel to the y-axis.

We now analyse the frequency dependence of the resonant peak voltage ΔV when applying $\boldsymbol{H_0}$ along the z-axis. For each value of the excitation frequency the static magnetic field was adjusted to keep the system at resonance, so that the mode excited by microwaves is the quasi-uniform FMR mode of the YIG sample. As seen in Fig. 2a, a nearly constant ΔV is observed for frequencies larger than 3.2 GHz. Surprisingly, below 3.2 GHz there is an abrupt increase in ΔV. To prove whether this increase is associated with increased microwave absorption power P_{abs}, which characterises the angular momentum transferred from the microwave field to the magnetic subsystem, we measured the frequency dependence of P_{abs} and show in Fig. 2b. The experimental data indicate that P_{abs} does not increase but rather decreases for f<3.2 GHz which can be explained by the reduction of magnetic susceptibility in YIG. Therefore, one can conclude that the observed increase of ΔV (and that of $\boldsymbol{j_s}$) is not due to the change of the microwave absorption. To take into account the frequency dependence of P_{abs} we introduce a parameter $\Delta V/P_{\text{abs}}$ that characterises the conversion efficiency of the angular momentum created by the microwave field into the spin current $\boldsymbol{j_s}$[14]. As seen in Fig. 2c, starting from f=3.2 GHz the conversion efficiency continuously increases with decreasing frequency. Similar experiments performed keeping the absorbed microwave power constant (see the inset of Fig. 2c) also demonstrate a clear enhancement of the ISHE voltage at f<3.2 GHz. Since the absorbed power is proportional to the injected angular momentum from the microwave, we can confirm that the reduction of P_{abs} is the origin of the decrease in ΔV observed below 3.0 GHz in Fig. 2a. These experimental findings suggest that for f<3.2 GHz the magnetic subsystem absorbs the angular momentum from a source different from the microwave field. In agreement with this assumption, the linear excitation theory describing the interaction of the magnetic subsystem with the microwave field[16-18] (see the supplementary information for more details) was found to be applicable to the

experimental data for f>3.2 GHz only (solid line in Fig. 2c). To characterise the observed enhancement at different applied microwave powers P, we analysed the ratio of ΔV measured at frequencies above (4GHz) and below (3GHz) the critical frequency 3.2 GHz as a function of P (Fig. 2d). The enhancement of ΔV is more efficient at low powers and gradually disappears with increasing P. Thus, the increase of ΔV can be attributed to a nonlinear spin-wave process (see more details in the Supplementary information).

In order to gain additional information about the magnetic subsystem, we used Brillouin light scattering (BLS) spectroscopy[19]. This technique is sensitive not only to the quasi-uniform FMR mode, but also to short-wavelength spin waves, which can be created due to the relaxation of magnetisation dynamics. Figure 3 shows the BLS intensity as a function of the excitation and detection frequencies. The data were obtained by maintaining the system at resonance and the detection frequency corresponds to the frequency of spin waves in the YIG layer. At the excitation frequencies above 3.2 GHz, the BLS spectrum shows peaks at the FMR frequency which is equal to the excitation frequency (solid line in the figure). At the lower excitation frequencies, however, a second group of spin waves appears in the spectrum, whose frequency is exactly one half of the excitation frequency (dashed line in the figure). These additional spin waves are created due to the three-magnon splitting process[13,20,21], representing a splitting of the quasi-uniform FMR mode into two short-wavelength spin waves of the half frequency as illustrated by the inset of Fig. 3. This process is only allowed if there are available spectral states at the frequency of the secondary spin waves. Due to the peculiarities of the spin-wave spectrum in ferromagnets[13], this condition is only met for relatively small static magnetic fields (therefore low excitation frequencies). Calculations based on the spin-wave theory in magnetic films[22] show that the three-magnon splitting is

allowed in YIG for the FMR frequencies below 3.15 GHz, which matches well the experimental value of the critical frequency 3.2 GHz.

These results reveal a clear correlation between the enhancement of the spin current observed at low frequencies and the three-magnon splitting process. The three-magnon splitting is well known[23] and usually considered as a parasitic effect, limiting the performance of conventional microwave electronic devices. In addition, in proposed spin-wave electronics[24] employing the inductive technique for detection of magnetisation oscillations, it is difficult to detect and use the short-wavelength secondary spin waves. By contrast, in spin current devices based on the angular momentum exchange at interfaces, both quasi-uniform FMR and short-wavelength spin waves contribute to the signal conversion. To understand the effect of the three-magnon splitting on the spin-current let us discuss the flow of angular momentum in the studied system illustrated in Fig. 4. It is important to emphasize that due to angular momentum conservation, any changes of magnetisation in a ferromagnet result in changes of the angular momentum accumulated in the magnetic subsystem. Thus, in order to change the magnetisation, one needs to create a corresponding flow of the angular momentum into the magnetic subsystem from an external source or from the lattice, as it happens by the Einstein-de Haas effect[25]. In the absence of three-magnon splitting (Fig.4a), the source of the angular momentum flow causing the excitation of the magnetisation precession is the flow from the microwave field $\mathfrak{T}_{MW}$. This precession leads to the reduction of the longitudinal magnetisation $\Delta M_{||}$. At equilibrium the flow from the microwave field is balanced by the flow of the angular momentum into the lattice $\mathfrak{T}_L$ due to the spin-lattice relaxation: $\mathfrak{T}_{MW} = \mathfrak{T}_L$. Using the Bloch equation[7], $\Delta M_{||}$ is expressed as $\Delta M_{||} = \gamma \mathfrak{T}_L T_1$, where T_1 is the spin-lattice relaxation time. In the presence of the Pt layer, we should take into account an additional flow due to the spin current $\boldsymbol{j}_s$ across the YIG/Pt interface, which is also

proportional to $\Delta M_{\parallel}$ [8,16-18], by replacing T_1 with an effective time T_1^* ($T_1^* < T_1$). Thus, the flow equilibrium between the microwave field, on one side, and the lattice and Pt layer, on the other side, defines the equilibrium value of $\Delta M_{\parallel}$ and therefore that of $\boldsymbol{j_s}$, both of which are proportional to T_1^*. We emphasize that the only source of the angular momentum is the microwave field and both $\boldsymbol{j_s}$ and ΔV are defined solely by the absorbed microwave power, since $\Delta M_{\parallel} \propto P_{abs}$.

The situation drastically changes when the three-magnon splitting is involved as illustrated in Fig. 4b. The quasi-uniform FMR mode excited by the microwave field creates short-wavelength spin waves due to the three-magnon splitting. Then both the quasi-uniform FMR and the spin waves transfer the angular momentum into the lattice and to the Pt layer. At first glance, it seems that the total flow equilibrium is not affected since the microwave field remains to be the only source of the angular momentum. However, this is only the case if the three-magnon splitting would conserve the total angular momentum of the magnetic subsystem. Following a simple picture of the three-magnon splitting, where one magnon emits two magnons, one can argue that this process increases the total number of magnons. In a standard quantisation scheme, one magnon carries the angular momentum of $\hbar$ [26] and therefore the three-magnon splitting does not conserve the total angular momentum of the magnetic subsystem. Accordingly, three-magnon splitting is forbidden, if the magnetic system is considered to be isolated, as in the model taking into account only the exchange interaction[26]. This restriction is removed by incorporating the magnetic dipole interaction in the model. In fact, the operator of the angular momentum of magnetic subsystem alone does not commute with the Hamiltonian describing the magnetic dipole interaction. In contrast, the operator of total angular momentum comprising both the magnetic subsystem and the lattice does commute with this Hamiltonian[27]. Since the three-magnon splitting requires the flow of

the angular momentum from the lattice, the flow between the lattice and the magnetic subsystem becomes bidirectional as shown in Fig. 4b. Therefore in the three-magnon splitting regime, the lattice serves as an additional source of angular momentum flow, which results in the increase of $\Delta M_{\parallel}$ and, consequently, in the enhancement of the spin current across the YIG/Pt interface.

Although the quantum theory of a ferromagnet with both the exchange and the magnetic dipole interactions exists since more than seventy years[28,29], a rigorous quantum consideration of the angular momentum exchange between the magnetic subsystem and the lattice due to the dipole interaction is still missing. Therefore, the quantitative description of the spin current enhancement due to three-magnon splitting is not possible at the moment. However, even a simple classical consideration of the three-magnon splitting (see the supplementary information) shows that this process indeed increases $\Delta M_{\parallel}$ and, as a consequence, enhances the spin current across the YIG/Pt interface. The observed enhancement of the spin-current could be also attributed to a higher efficiency to generate spin currents into the normal metal by short-wavelength spin waves than that by the homogenous FMR mode. However, our experiments on excitation of short-wavelength spin waves directly using nonlinear parametric pumping which are in agreement with results of another group[30] preclude this possibility.

We show that the three-magnon splitting in a magnetic insulator, due to angular momentum transfer from the lattice, enhance spin-current emission in the YIG/Pt interface. This spin current enhancement is controlled by changing the frequency and the external magnetic field. These findings shed new light onto the role of nonlinear magnetic dynamics and spin waves in spintronics. In particular, the short-wavelength spin waves, usually considered to be unimportant in conventional microwave electronics, are shown to have potential for spintronic applications. From a fundamental point of view, our findings clearly demonstrate

the importance of the magnetic dipole interaction for the exchange of the angular momentum between magnetic and nonmagnetic subsystems, and also the importance of the angular momentum conservation law for analysis of magnetic dynamics.

Methods

The monocrystalline YIG film with the thickness of 5.1 μm was grown on a gallium gadolinium garnet substrate and a 15 nm-thick Pt layer was sputtered on top of the YIG film. The lateral dimensions of the sample were 1.5×5 mm. The independently measured Gilbert damping constant of the YIG film was 10^{-4}. As shown in Fig. 1a, the sample was attached to a standard 0.5-mm-wide 50 Ω microstrip transmission line used for broadband excitation of magnetic dynamics in the YIG film. The excited quasi-uniform FMR mode expands over the entire YIG film due to the low damping characteristic. The experimental structure was placed into a static magnetic field, $\boldsymbol{H}_0$, which can be aligned in the plane or perpendicular to the plane of the YIG film. For spin current detection by the ISHE, two electrodes were attached to the Pt layer 3.5 mm apart from each other. The electric detection is sensitive to the electric field induced in Pt along the y-direction. All the measurements were performed at room temperature.

The magnetisation dynamics in the YIG film was studied by two complementary techniques. The quasi-uniform FMR mode was characterised by conventional electronic measurements using the network analyser. The information about the microwave power absorbed in the YIG film was measured from simultaneous measurements of the power reflected from and transmitted through the microstrip transmission line. In addition, we used BLS spectroscopy

in the quasi-backward scattering geometry[19] to access short-wavelength spin waves created in the YIG film as a result of the magnon-magnon relaxation of the directly excited quasi-uniform FMR mode.

Additional information

The authors declare no competing financial interests. Supplementary information accompanies this paper on www.nature.com/naturematerials. Reprints and permissionsinformation is available online at http://www.nature.com/reprints. Correspondence andrequests for materials should be addressed to H. K.

Acknowledgements

The authors thank A. Slavin, E. Saitoh, K. Ando, K. Harii and Y. Tserkovnyak for their valuable discussions. H. K. is grateful to the Royal Society for their financial support via TG102227. S.D. acknowledges helpful discussion with B. Koopmans on conservation of angular momentum in ferromagnets. Work in Münster has been supported by the Deutsche Forschungsgemeinschaft and by the European Union through the STREP Project Master NMP3-SL-2008-212257.

Author contributions

Sample preparation: H. K., O. D. & D. F.; measurement and data analysis: O. D., H. K. & V.E.D.; interpretation and theoretical calculation: S. O. D. & H. K.; manuscript writing: S. O. D., H. K., V. E. D. & A. J. F. This project was initiated and managed by H. K. & S. O. D.

References

[1] Maekawa, S. *Concepts in Spin Electronics* (Oxford University Press, Oxford, 2006).

[2] Johnson, M. & Silsbee, R. H. Interfacial charge-spin coupling: Injection and detection of spin magnetization in metals. *Phys. Rev. Lett.* **55**, 1790–1793 (1985).

[3] Jedema, F. J., Filip, A. T. & van Wees, B. J. Electrical spin injection and accumulation at

room temperature in an all-metal mesoscopic spin valve. *Nature* **410**, 345–348 (2001).

[4] Lou, X. *et al.* Electrical detection of spin transport in lateral ferromagnet-semiconductor devices. *Nature Phys.* **3**, 197–202 (2007).

[5] Yang, T., Kimura, T. & Otani, Y. Giant spin-accumulation signal and pure spin-current-induced reversible magnetization switching. *Nature Phys.* **4**, 851-854 (2008).

[6] Slachter, A., Bakker, F. L., Adam, J.-P. & van Wees, B. J. Thermally driven spin injection from a ferromagnet into a non-magnetic metal. *Nature Phys.* **6**, 879-882 (2010).

[7] Saitoh, E., Ueda, M., Miyajima, H. & Tatara G. Conversion of spin current into charge current at room temperature: inverse spin-Hall effect. *Appl. Phys. Lett*. **88**, 182509 (2006).

[8] Kajiwara, Y. *et al.* Transmission of electrical signals by spin-wave interconversion in a magnetic insulator. *Nature* **464**, 262–266 (2010).

[9] Kittel, C. *Introduction to Solid State Physics Seventh Edition* (John Wiley & Sons, New York, 1996).

[10] Kato, Y. K., Myers, R. C., Gossard, A. C. & Awschalom, D. D. Observation of the Spin Hall Effect in Semiconductors. *Science.* **306**, 1910-1913 (2004).

[11] Wunderlich, J., Kaestner. B., Sinova, J. & Jungwirth, T. Experimental observation of the spin-Hall effect in a two-dimensional spin-orbit coupled semiconductor system. *Phys. Rev. Lett.* **94** 047204 (2005).

[12] Takahashi, S. & Maekawa, S. Spin current, spin accumulation and spin Hall effect. *Sci Technol. Adv. Mater*. **9** 014105 (2008).

[13] Gurevich, A. G. & Melkov, G. A. *Magnetization oscillations and waves* (CRC, New York, 1994).

[14] Sandweg, C. W., Kajiwara Y., Ando, K., Saitoh, E. & Hillebrands, B. Enhancement of the spin pumping efficiency by spin wave mode selection. *Appl. Phys. Lett*. **97** 252504 (2010).

[15] Kittel, C. On the theory of ferromangetic resonance absorption. *Phys. Rev.* **73** 155 (1948).

[16] Tserkovnyak, Y. & Brataas, A. Enhanced Gilbert damping in thin ferromagnetic films. *Phys. Rev. Lett.* **88**, 117601 (2002).

[17] Tserkovnyak, Y., Brataas, A., & Bauer, G. E. Dynamic stiffness of spin valves. *Phys. Rev. B*, **67** 140404 (2003).

[18] Ando, K. & Saitoh, E. Inverse spin-Hall effect in palladium at room temperature. *J. Appl. Phys*. **108** 113925 (2010).

[19] Demokritov, S. O., Hillebrands, B. & Slavin, A. N. Brillouin light scattering studies of confined spin waves: linear and nonlinear confinement. *Phys.Rep.* **348**, 441-489 (2001).

[20] Ordóňez-Romero, C. L. *et al*. Three-magnon splitting and confluence processes for spin-wave excitations in yttrium iron garnet films: Wave vector selective Brillouin light scattering measurements and analysis. *Phys. Rev. B* **79**, 144428 (2009).

[21] Schultheiss, H. et al. Direct Current Control of Three Magnon Scattering Processes in Spin-Valve Nanocontacts. *Phys. Rev. Lett.* **103**, 157202 (2009).

[22] Kalinikos, B. A. & Slavin, A. N. Theory of dipole-exchange spin wave spectrum for

ferromagnetic films with mixed exchange boundary conditions. *Phys. C* **19**, 7013-7033 (1986).

[23] Wigen, P. E. *Nonlinear Phenomena and Chaos in Magnetic Materials* (World Scientific, Singapore, 1994).

[24] Khitun, A., Bao, M. & Wang, K. L. Spin wave magnetic nanofabric: a new approach to spin-based logic circuity. IEEE Trans. Mag. 44 2141-2151 (2008).

[25] Einstein, A. & de Haas, W. J.TITLE Verhandlungen, Deutsche Phys. Gesellsehaft **17**, 152 (1915).

[26] Bloch, F. Zur Theorie des Ferromagnetismus, *Z. Phys.* **61** 206-219 (1930).

[27] Bloembergen, N.S., Shapiro, P.S. Pershan & O. Artman. Cross-relaxation in spin systems. Phys. Rev. **114**, 445-459 (1959).

[28] Holstein, T. & H. Primakoff, Field dependence of the intrinsic domain magnetization of a ferromagnet. Phys. Rev. 58, 1098-1113 (1940).

[29] Majlis, N. *THE QUANTUM THEORY OF MAGNETISM Second Edition*, (World Scientific Publishing, Singapore 2007).

[30]. Sandweg C.W., Kajiwara Y., Chumak A.V, Serga A.A., Vasyuchka V.I., Jungfleisch M.B., Saitoh E., Hillebrands B. "Spin pumping by parametrically excited exchange magnons" accepted by Phys. Rev. Lett.

Figure captions

Figure 1: Ferromagnetic resonance and spin current detection in YIG/Pt layered system.

a, Schematic layout of the experimental set-up. Ferromagnetic resonance in the YIG layer is excited using a microwave current flowing in a microstrip transmission line. $\boldsymbol{H}_0$ denotes the applied static magnetic field. Electrodes attached to the Pt film are used to detect the voltage induced in the film due to the spin current flow; **b**, Ferromagnetic resonance in YIG at f=5 GHz detected via microwave absorption for $\boldsymbol{H}_0 \| \mathbf{z}$. H_{res} defines the resonance field; **c,** Frequency dependence of H_{res} for $\boldsymbol{H}_0 \| \mathbf{z}$, the dots illustrate experimental data and the solid curve is calculated based on the Kittel formula; **d,** Field dependence of the induced voltage measured at different orientations of $\boldsymbol{H}_0$ as labeled. ΔV indicates the peak value of V at H_{res}.

Figure 2: The frequency and power dependence of the ISHE voltage and the microwave absorption in YIG.

a, Frequency dependence of the peak voltage at resonance conditions. Note that an abrupt increase of ΔV is observed at f<3.2 GHz where we insert the red dash line. **b**, Frequency dependence of the absorbed microwave power. A strong decrease of P_{abs} starts at f=3.2 GHz. **c,** Frequency dependence of the ratio $\Delta V/P_{abs}$ which characterises the conversion efficiency of the angular momentum absorbed from microwaves into spin current, measured at a constant power of microwave excitation. A strong increase of $\Delta V/P_{abs}$ starts at f=3.2 GHz. The solid line is the result of calculations based on the linear excitation theory. The inset shows the results of similar measurements performed by keeping the absorbed microwave power (P_{abs}) constant; **d**, Power dependence of the spin current enhancement, characterised by the ratio of the values of ΔV measured 3.0 and 4.0 GHz. Strong power dependence indicates that a nonlinear process is behind the enhancement.

Figure 3: Spin waves created by the three-magnon splitting measured using BLS.

Pseudo-colour two-dimensional plot of the BLS intensity as a function of the excitation and detection frequencies (f and f_{BLS}). The intensity is proportional to the squared amplitude of the FMR mode or to the spin-wave intensity. For each excitation frequency, the applied magnetic field has been adjusted to fulfil the resonance conditions. The solid line indicates the condition of $f_{BLS}= f$, whereas the dash line corresponds to that of $f_{BLS}=f/2$. Note that spin waves with the half frequency appear only for f <3.2 GHz. The inset is the spin-wave spectrum in YIG with a schematic of the three-magnon splitting. The upper and lower boundaries of the spin-wave manifold correspond to the spin waves propagating perpendicular and parallel to the applied field, as labelled.

Figure 4: Schematics of angular momentum flows in the YIG/Pt layered system.

In these figures, FMR is used to denote quasi-uniform FMR mode that we excite using the microwave. **a,** In the case without three-magnon splitting. The external microwave field excites the quasi-uniform FMR mode by transferring the angular momentum into the magnetic subsystem of YIG, $\mathfrak{T}_{MW}$. This flow is directed to the lattice due to the spin-lattice relaxation in YIG $\mathfrak{T}_{L}$, and induces a spin current across the YIG/Pt interface $\boldsymbol{j}_{\mathrm{S}}$. The amplitude of the magnetic precession, which is proportional to $\boldsymbol{j}_{\mathrm{S}}$, is determined by the equilibrium between the three flows. **b**, In the case that three-magnon splitting is allowed. Due to the three-magnon process the quasi-uniform FMR mode is split into secondary spin waves. To support the splitting, an additional reverse flow of angular momentum from the lattice to the magnetic subsystem is created, which enhances the spin current across the YIG/Pt interface (indicated by red arrows). Under these conditions, $\boldsymbol{j}_{s}$ is determined by both the amplitude of the quasi-uniform FMR mode and that of secondary spin-waves.

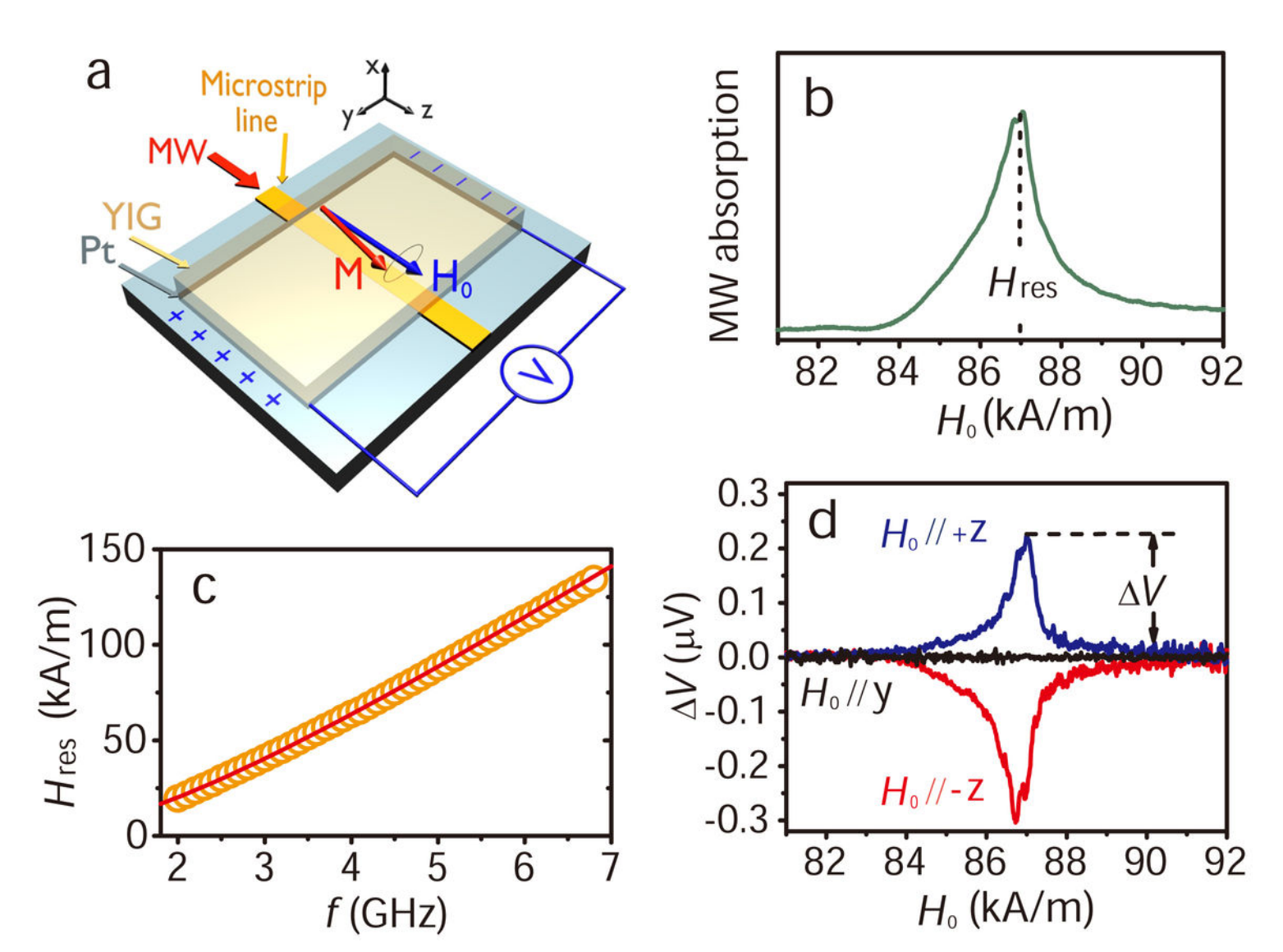
a
Microstrip line
MW
YIG
Pt
M
H_0
x
y
z
V
b
MW absorption
H_{res}
82
84
86
88
90
92
H_0 (kA/m)
c
150
100
50
0
H_{res} (kA/m)
2
3
4
5
6
7
f (GHz)
d
H_0 // +z
ΔV
H_0 // y
H_0 // -z
0.3
0.2
0.1
0.0
-0.1
-0.2
-0.3
ΔV (μV)
82
84
86
88
90
92
H_0 (kA/m)

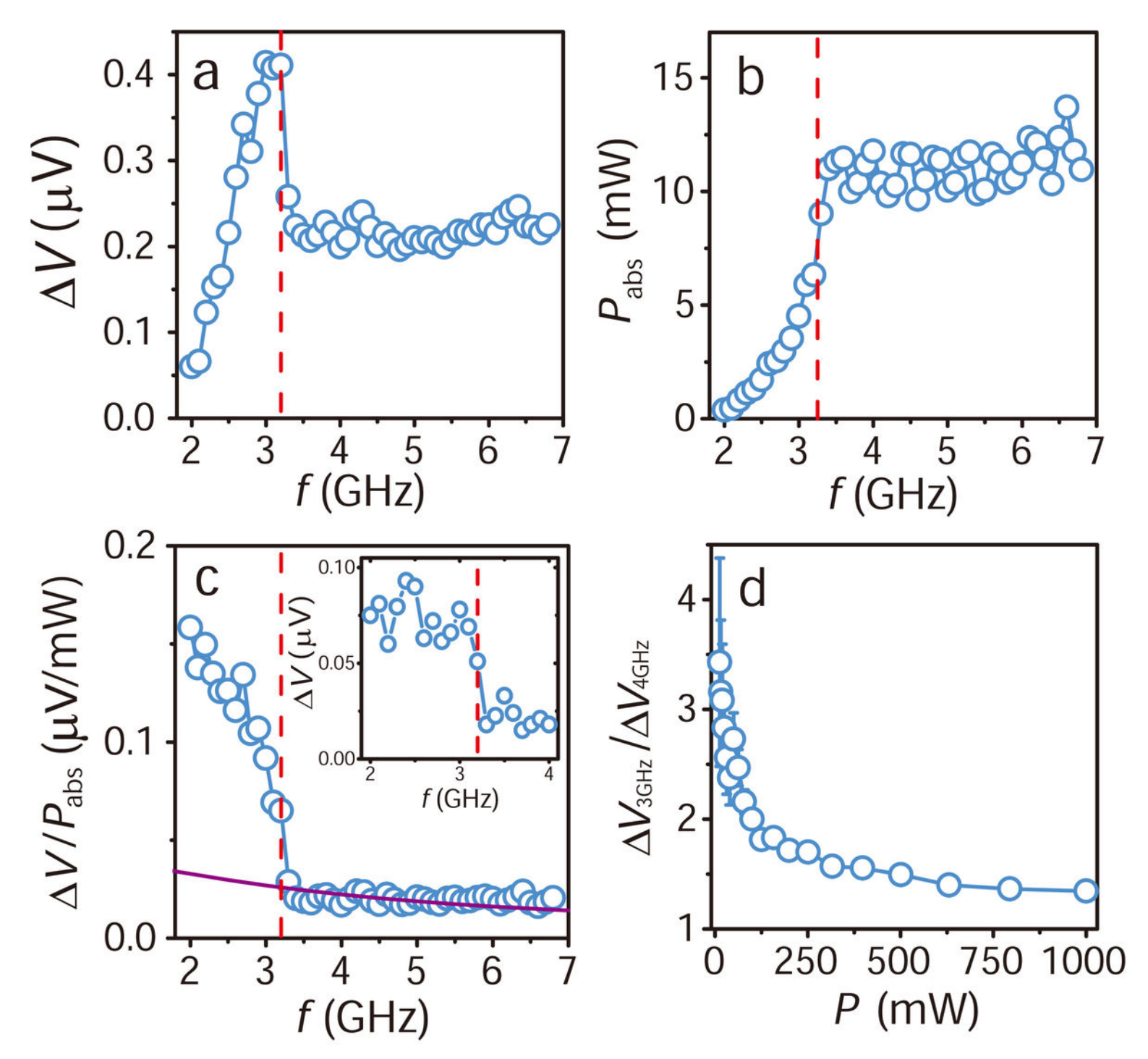
a
b
c
d
ΔV (μV)
f (GHz)
P_abs (mW)
ΔV/P_abs (μV/mW)
ΔV_3GHz /ΔV_4GHz
P (mW)

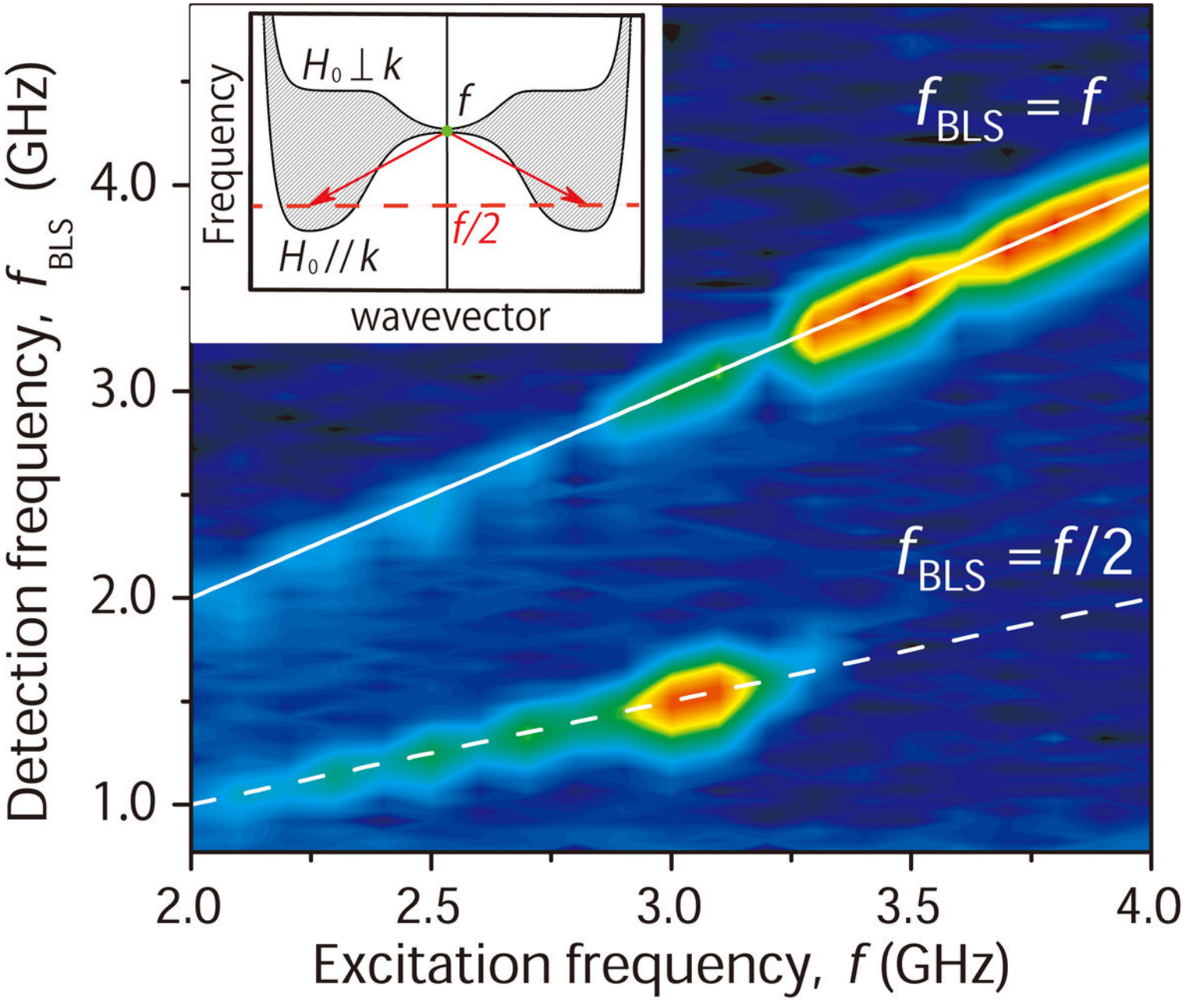
Detection frequency, f_{BLS} (GHz)
Excitation frequency, f (GHz)
$f_{BLS} = f$
$f_{BLS} = f/2$
Frequency
wavevector
$H_0 \perp k$
$H_0 // k$
f
$f/2$
1.0
2.0
3.0
4.0
2.0
2.5
3.0
3.5
4.0

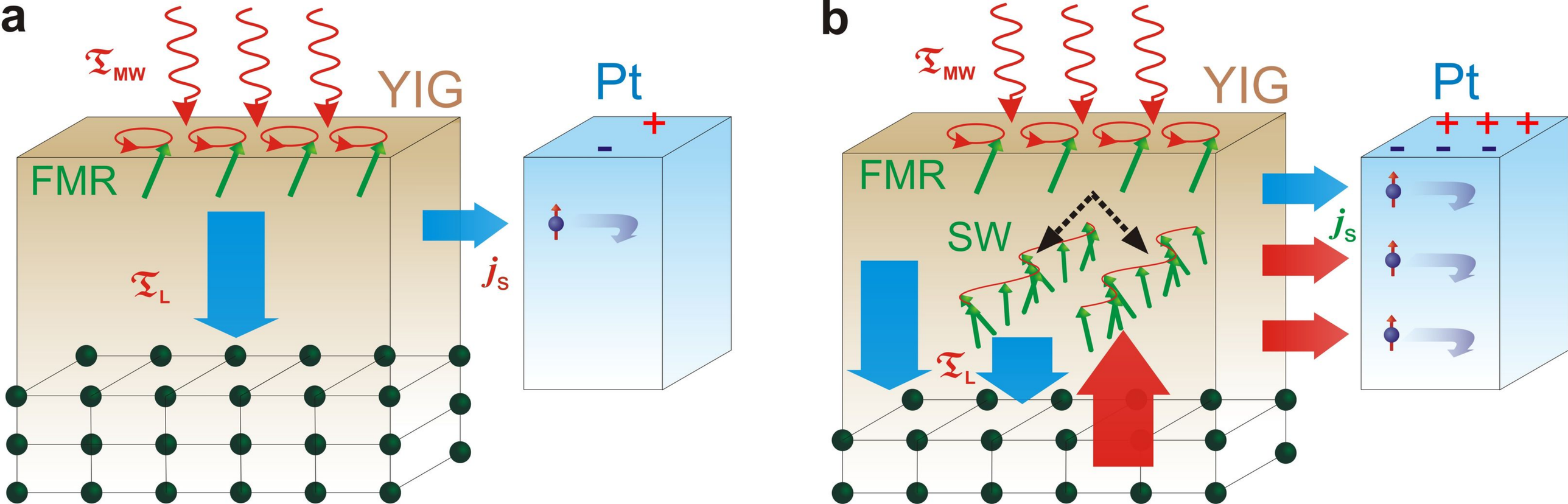
a
$\mathcal{T}_{MW}$
YIG
Pt
FMR
$\mathcal{T}_L$
j_S
+
-
b
$\mathcal{T}_{MW}$
YIG
Pt
FMR
SW
$\mathcal{T}_L$
j_S
+ + +
- - -